Independent Thallium-201 Accumulation and Fluorine-18-Fluorodeoxyglucose Metabolism in Glioma

Noboru Oriuchi, Katsumi Tomiyoshi, Tomio Inoue, Khalil Ahmad, Muhammad Sarwar, Mari Tokunaga, Hideki Suzuki, Naoyuki Watanabe, Tsuneo Hirano, Satoru Horikoshi, Takashi Shibasaki, Masaru Tamura and Keigo Endo

Departments of Nuclear Medicine and Neurosurgery, Gunma University School of Medicine, Gunma; and Department of Neurosurgery, National Center Hospital for Mental, Nervous and Muscular Disorders, National Center of Neurology and Psychiatry, Tokyo, Japan

SPECT with ^{201}Tl is an effective procedure for evaluating the malignancy of glioma. Our goal was to investigate the diagnostic relevance of both ^{201}Tl SPECT and [^{18}F]fluorodeoxyglucose (FDG) PET and the relation between ^{201}Tl uptake and glucose metabolism in glioma using comparative SPECT and PET studies. **Methods:** Thallium-201 SPECT and FDG dynamic PET studies were performed in 20 patients with untreated glioma (5 with glioblastoma, 5 with anaplastic glioma, 10 with low-grade glioma). Thallium-201 uptake in the tumor was estimated using the ^{201}Tl index, defined as the ratio of ^{201}Tl uptake in the tumor to that in the contralateral normal brain on SPECT images obtained 15 min after intravenous injection. We measured regional glucose metabolic parameters, including rate constants and regional cerebral metabolic rate of glucose utilization (rCMRgl), in the tumor. We then compared the regional ^{201}Tl index and glucose metabolic parameters with the histologic characteristics, malignancy and computed tomographic/magnetic resonance imaging findings. In addition, we investigated the correlation between the ^{201}Tl index and glucose metabolic parameters. **Results:** Thallium-201 SPECT showed abnormal ^{201}Tl uptake in all patients with glioblastoma and anaplastic glioma. Thallium-201 indices of glioblastoma (202.6 ± 22.1%) and anaplastic glioma (176.6% ± 26.6%) were significantly higher than that for low-grade glioma (106.7% ± 13.8%). The rCMRgl value of glioblastoma (17.6 ± 3.5 μmole/100 g/min) was also significantly higher than that for low-grade glioma (10.8 ± 4.5 μmole/100 g/min), although rCMRgl showed a large variability in both high- and low-grade glioma. Rate constants of FDG kinetics had no correlation with histological grade of glioma. Some patients with high-grade glioma, however, showed false-negative results with FDG-PET because of high normal brain uptake of FDG. Conversely, most low-grade glioma could not be localized by ^{201}Tl SPECT. There was no correlation between the ^{201}Tl index and glucose metabolic parameters. **Conclusion:** Thallium-201 indices and rCMRgl values for glioblastoma were higher than those for low-grade glioma. Thallium-201 uptake in the tumor may be independent of increased glucose transport or metabolism. Thallium-201 SPECT and FDG-PET are complementary in the diagnosis of glioma, although ^{201}Tl SPECT is more significantly correlated with the malignancy of glioma.

Key Words: thallium-201; SPECT; fluorine-18-fluorodeoxyglucose; PET; glioma

J Nucl Med 1996; 37:457–462

Many investigators have reported the usefulness of ^{201}Tl for the diagnosis of brain tumor as well as lung and thyroid cancer (*1–6*). The clinical utility of ^{201}Tl SPECT in brain tumor has mainly focused on the differentiation between malignant and benign glioma, on the detection of residual neoplastic tissue after therapy and on the early detection of recurrence or malignant transformation of glioma (*7–10*). We previously reported a significant correlation between ^{201}Tl uptake and the proliferative activity of tumor cells in vivo and the prognosis of patients with glioma (*7*). Although the mechanism of ^{201}Tl accumulation in neoplastic lesions is uncertain, blood flow, diffusibility of the tracer through vessels and Na^+-K^+ adenosine triphosphatase activity are all considered factors that affect its uptake (*11–13*). Thallium-201 uptake may be related to cell growth rates (*14,15*), but the factor most essential to accumulation of ^{201}Tl in neoplastic lesions remains to be elucidated. Therefore, the clinical usefulness of ^{201}Tl SPECT in the diagnosis of brain tumor has not been definitively determined.

Fluorine-18-fluorodeoxy-D-glucose (FDG) PET has also been used in the diagnosis of brain tumor. Many investigators have shown the value of FDG-PET in evaluating degree of malignancy, prognosis in patients and tumor recurrence after surgical or radiation therapy (*16–21*).

To clarify the utility of ^{201}Tl SPECT and FDG-PET for the diagnosis of glioma, we compared ^{201}Tl uptake in the tumor with regional cerebral transport and metabolic rates of utilization of glucose (rCMRgl) using FDG-PET studies. In the present study, we performed dynamic FDG-PET studies and calculated rCMRgl using measured rate constants because the regional rate constants and rCMRgl in brain tumor seem to be different from those in the normal brain. The rCMRgl in the normal brain has generally been calculated using fixed rate constants measured in normal volunteers by autoradiography (*22–24*).

MATERIALS AND METHODS

Patients

Twenty consecutive patients (16 men, 4 women; aged 24–65 yr; mean age 45.2 yr) with gliomas underwent ^{201}Tl SPECT and FDG-PET studies at Gunma University Hospital from June 1989 to December 1993. Computed tomography (CT) or magnetic resonance imaging (MRI) was performed in all patients to evaluate localization and enhancement of the tumor. Histological findings were glioblastoma in 5 patients; anaplastic glioma, including anaplastic astrocytoma and oligoastrocytoma, in 5; and low-grade glioma, including low-grade astrocytoma and oligoastrocytoma, in 10. No patient received previous therapy for their brain tumor. The aim and methods of the study were explained and all patients gave informed consent.

Thallium-201 SPECT Studies

Thallium-201 SPECT studies were performed using a ring-type SPECT instrument 15 min after intravenous injection of 111 MBq ^{201}Tl-chloride. Static images were reconstructed using a Butter-

Received Jan. 3, 1995; revision accepted July 30, 1995.

For reprints contact: Keigo Endo, MD, Department of Nuclear Medicine, Gunma University School of Medicine, 3-39-22 Showa-machi, Maebashi, 371 Japan.

worth and Ramachandran filter according to data acquired at 8.3 min for each plane. Three to six different imaging planes, including tumor site, were used in all patients. Tumor uptake of ^{201}Tl was evaluated by the ^{201}Tl index, as reported previously (*7*). In brief, 4 × 4-pixel regions of interest (ROIs) were placed in the tumor and contralateral normal sites on the cathode ray tube. If there was no significant ^{201}Tl uptake in the tumor, ROIs were placed by using CT or MRI for reference. The ^{201}Tl index was defined as the ratio of average counts in the tumor to those in the normal site.

FDG-PET Studies

PET studies were performed using a PCT-H1 positron CT (Hitachi Corp., Tokyo, Japan). Intravenous FDG (200 MBq) injection was followed by consecutive data acquisition every 2 min for 60 min to reconstruct the images of seven planes at 16-mm intervals. Spatial resolution at the center of the field was 7 mm (FWHM), and the slice thickness was 8 mm. Arterial blood sampling was performed every 15 sec for 2 min, every 30 sec for 3 min, every 1 min for 5 min, every 2–5 min for 20 min and every 10 min for 30 min after the FDG bolus injection. Plasma radioactivities were measured to determine the time-activity curve of FDG. Plasma glucose concentration in the arterial blood was measured four times during the study. To calculate the regional mean values of ^{18}F, ROIs were placed at sites corresponding to the ROIs used for measuring the ^{201}Tl index on the SPECT studies.

Measurement of Rate Constants in Neoplastic Lesions

According to the three-compartment model, the regional mean value of ^{18}F at time t is determined as follows (*22,24*):

$$Ci^*(t) = [(p_1 \exp(-q_1 t) + p_2 \exp(-q_2 t)] \otimes Cp^*(t), \quad \text{Eq. 1}$$

where

$$p_1 = k_1^*/(a_2 - a_1) \times (k_3^* + k_4^* - a_1),$$

$$p_2 = k_1^*/(a_2 - a_1) \times (a_2 - k_3^* - k_4^*),$$

$$q_1 = a_1 = \tfrac{1}{2}\{k_2^* + k_3^* + k_4^* - r[(k_2^* + k_3^* + k_4^*)^2 - 4k_2^*k_4^*]\},$$

$$q_2 = a_2 = \tfrac{1}{2}\{k_2^* + k_3^* + k_4^* + r[(k_2^* + k_3^* + k_4^*)^2 - 4k_2^*k_4^*]\},$$

and $Cp^*(t)$ denotes plasma ^{18}F radioactivity in the arterial plasma at time t; and ⊗ denotes a convolution function. From these equations, the regional rate constants k_1^*, k_2^*, k_3^* and k_4^* in a three-compartment model were determined using $Cp^*(t)$ and the regional cerebral mean values of ^{18}F ($Ci^*(t)$) according to Equation 1:

$$k_1^* = p_1 + p_2,$$

$$k_2^* = p_1q_1 + p_2q_2/p_1 + p_2,$$

$$k_3^* = p_1p_2(q_1 - q_2)^2/(p_1 + p_2)(p_1q_1 + p_2q_2),$$

$$k_4^* = q_1q_2(p_1 + p_2)/p_1q_1 + p_2q_2.$$

In the present study, the plasma radioactivity of ^{18}F was approximated from measurements of $Cp^*(t)$ at intervals using a spline function, and fixed rate constants reported by Phelps et al. (*22*) were used to derive the calculated $Ci^*(t)$. Using the linear least-squares method, p_1 and p_2 were first fitted to minimize the difference between the calculated $Ci^*(t)$ and the measured $Ci^*(t)$, and the resultant rate constants were used instead of the fixed rate constants to derive the optimal p_1, p_2, q_1 and q_2 using the nonlinear least-squares method. The optimal p_1, p_2, q_1 and q_2 were used to calculate k_1^*, k_2^*, k_3^* and k_4^*. The optimization criteria were met when the summation of the square of the error became constant.

Measurement of rCMRgl in Neoplastic Lesions

Using the rate constants previously derived, the plasma glucose concentration (Cp) and the lumped constant (LC), rCMRgl was determined by the reported previously equation (*22,24*):

$$rCMRgl = Cp/LC \times k_1^*k_3^*/(k_2^* + k_3^*),$$

where LC = 0.418.

Statistical Analysis

To compare the mean indices among patients with glioblastoma, anaplastic glioma and low-grade glioma, statistical comparison was performed using the unpaired Student's t-test.

RESULTS

Thallium-201 uptake by the tumor was higher in patients with high-grade glioma, including glioblastoma and anaplastic glioma, than in patients with low-grade glioma (Table 1). Thallium-201 indices for glioblastoma and anaplastic glioma were 202.6% ± 22.1% and 176.6% ± 26.6%, respectively, significantly higher than that for low-grade glioma (106.7 ± 13.8%; $p < 0.001$ versus glioblastoma; $p < 0.01$ versus anaplastic glioma) (Table 2). Two patients (Patients 11 and 12) with low-grade glioma showed definite uptake of ^{201}Tl at the tumor sites; however, both died, one of lupus pneumonitis (Patient 11) and the other of malignant transformation (Patient 12). The other eight patients showed no abnormal ^{201}Tl uptake in the tumor.

Rate constant k_1^* values obtained by FDG dynamic PET studies tended to be high in patients with high-grade glioma (0.498 ± 0.168 min^{-1} for glioblastoma, 0.603 ± 0.362 min^{-1} for anaplastic glioma) and in those with low-grade glioma (0.392 ± 0.093 min^{-1}), but these values were not statistically significant (Table 2). Rate constants k_2^*, k_3^* and k_4^* also showed no significant differences in histological grade of glioma.

Tumor rCMRgl values were variable and higher in patients with glioblastoma than in those with low-grade glioma (17.6 ± 3.5 versus 10.8 ± 4.5 μmole/100 g/min, $p < 0.05$) (Table 2). In patients with anaplastic glioma, rCMRgl values were variable but not statistically different from those in patients with glioblastoma or low-grade glioma. Of five patients with anaplastic glioma, two (Patients 6 and 7) had high ^{201}Tl index and rCMRgl values and had a solid tumor with marked contrast enhancement on CT and MRI, and three (Patients 8–10) had low ^{201}Tl index and rCMRgl values and had a tumor with central necrosis and enhanced rim. Patient 6 had a markedly high k_1^* value, indicating increased glucose transport.

Of five patients with glioblastoma, four (Patients 1, 2, 4 and 5) had a tumor with central necrosis and an enhanced rim on CT and MRI (Fig. 1), and one (Patient 3) had a solid tumor with inhomogeneous enhancement, indicating multiple small necrotic foci in the tumor (Fig. 2). As shown in Figure 1 (Patient 2), ^{201}Tl SPECT was superior to FDG-PET in delineating the tumor. In some patients, findings were similar for ^{201}Tl SPECT and FDG-PET (Fig. 2).

Of 10 patients with low-grade glioma, four (Patients 11, 12, 16 and 17) had relatively high rCMRgl values: Patient 11 with central necrosis and an enhanced rim on CT and MRI demonstrated a relatively high ^{201}Tl index of 136% and an rCMRgl value of 11.6 μmole/100 g/min; another (Patient 12) with enhanced tumor demonstrated a ^{201}Tl index of 124% and an rCMRgl value of 12.9 μmole/100 g/min; and two others (Patients 16 and 17) had a tumor on CT and MRI but not on FDG-PET because the tumor was not delineated from normal brain (Fig. 3). The other six patients had lower rCMRgl values in the lesion than in the surrounding normal brain (Fig. 4).

TABLE 1
Clinical Features and Thallium-201 SPECT and FDG-PET Measurements

Pt. no.	Age (yr)	Sex	Location	Size (mm)	Histological finding	CT/MRI findings: Cyst necrosis	CT/MRI findings: CE	^{201}Tl index (%)	k_1^* (min^{-1})	k_2^* (min^{-1})	k_3^* (min^{-1})	k_4^* (min^{-1})	rCMRgl (μmole/100 g/min)	Survival after SPECT study (mo)
1	35	M	L. parietal	39 × 34	Glioblastoma	+	+ (ringlike)	228	0.321	0.168	0.026	0.0053	12.3	40
2	56	M	L. parietal	50 × 45	Glioblastoma	+	+ (ringlike)	220	0.335	0.156	0.040	0.0058	17.2	19
3	20	M	R. thalamus	48 × 44	Glioblastoma	±*	+	203	0.544	0.161	0.033	0.0055	21.8	7 d
4	62	M	L. parietal	63 × 30	Glioblastoma	+	+ (ringlike)	187	0.573	0.171	0.023	0.0052	16.9	6
5	48	M	R. thalamus	46 × 38	Glioblastoma	+	+ (ringlike)	175	0.716	0.170	0.024	0.0052	19.6	17
6	44	M	R. thalamus	27 × 20	Anaplastic glioma	+†	+	205	1.245	0.168	0.025	0.0053	41.4	>26
7	43	F	L. frontal	40 × 30	Anaplastic glioma	−	+	205	0.451	0.157	0.036	0.0056	18.7	>63
8	49	M	C. callosum	42 × 29	Anaplastic glioma	+	+ (ringlike)	167	0.401	0.182	0.012	0.0049	7.7	4
9	38	M	L. frontal	81 × 37	Anaplastic glioma	+	+ (ringlike)	156	0.515	0.179	0.015	0.0050	9.7	>25
10	65	F	R. frontal	37 × 16	Anaplastic glioma	+	+ (ringlike)	150	0.404	0.183	0.011	0.0048	5.8	>31
11	42	F	R. basal ggl.	37 × 23	Low-grade glioma‡	+	+ (ringlike)	136	0.380	0.170	0.024	0.0052	11.6	3
12	24	M	Vermis	16 × 11	Low-grade glioma	−	+	124	0.531	0.175	0.019	0.0051	12.9	22
13	26	M	L. temp.-occip.	41 × 38	Low-grade glioma	−	−	111	0.255	0.158	0.035	0.0056	9.1	>64
14	60	F	L. thalamus	36 × 19	Low-grade glioma	−	−	105	0.441	0.183	0.011	0.0048	6.0	11
15	40	F	L. cerebellum	27 × 20	Low-grade glioma	−	±	104	0.442	0.171	0.023	0.0051	10.0	>37
16	40	F	L. frontal	36 × 26	Low-grade glioma	−	±	101	0.370	0.162	0.032	0.0055	14.1	31
17	54	M	L. temporal	23 × 19	Low-grade glioma	−	−	100	0.376	0.144	0.048	0.0061	21.2	>56
18	59	M	L. frontal	33 × 20	Low-grade glioma	−	±	100	0.456	0.181	0.013	0.0049	6.9	>20
19	40	M	R. frontal	32 × 29	Low-grade glioma	−	−	97	0.439	0.175	0.019	0.0051	9.4	>31
20	58	M	L. putamen	56 × 36	Low-grade glioma	+	−	89	0.227	0.171	0.023	0.0052	6.6	>59

*Small necrotic areas seen in solid tumor.
†Lateral portion of tumor is solid.
‡Diagnosed by stereotactic biopsy specimen.
C. = corpus; d = days; F = female; ggl. = ganglia; k_1^*, k_2^*, k_3^*, k_4^* = rate constants in FDG kinetic model; temp.-occip. = temporo-occipital; − = absent; + = present; ± = slightly visualized contrast enhancement (CE).

There was no statistical correlation between ^{201}Tl index and rCMRgl values in the 20 patients examined.

DISCUSSION

The present study revealed that ^{201}Tl index and rCMRgl values in patients with glioblastoma were higher than in those with low-grade glioma. Thallium-201 uptake in the tumor may be independent of increased glucose transport or metabolism, and no significant correlation was observed between ^{201}Tl uptake and FDG kinetics in tumors of patients with glioma. As reported previously (*7–10,17*), ^{201}Tl uptake was significantly increased in patients with high-grade than low-grade glioma. In the present study, the ^{201}Tl index of high- and low-grade gliomas ranged from 150 to 228 (mean value 189.6) and from 89 to 136 (mean value 106.7), respectively, and no overlap of the ^{201}Tl index value was observed between high- and low-grade gliomas, although the ^{201}Tl index values in the present study were lower than those reported previously by other investigators (*8,9,25*). These differences may be due to differences in patients, instruments, attenuation-correction methods and ROI sizes. We used a ring-type camera, with attenuation correction determined by phantom data acquisition, and 4 × 4-pixel ROIs, whereas others used a single-head camera and attenuation correction of 0.12/cm. We also found that the ^{201}Tl index of the glioma correlated well with the rate of tumor proliferation and the survival rate of the patients (*7*). These findings indicate the potential of ^{201}Tl SPECT for predicting the malignancy of glioma.

TABLE 2
Thallium-201 SPECT and FDG-PET Measurements According to Histological Grade

Histological finding	^{201}Tl index (%)	k_1^* (min^{-1})	k_2^* (min^{-1})	k_3^* (min^{-1})	k_4^* (min^{-1})	$k_1^*k_3^*/(k_2^* + k_3^*)$ (min^{-1})	$k_1^*/(k_2^* + k_3^*)$	rCMRgl (μmole/100 g/min)
Glioblastoma	202.6*	0.498	0.165	0.029	0.0054	0.072	2.57	17.6†
(5 patients)	(22.1)	(0.168)	(0.006)	(0.007)	(0.00003)	(0.020)	(0.87)	(3.5)
Anaplastic glioma	176.6‡	0.603	0.174	0.020	0.0051	0.048	3.11	16.5
(5 patients)	(26.6)	(0.362)	(0.011)	(0.011)	(0.00003)	(0.020)	(1.87)	(14.3)
Low-grade glioma	106.7	0.392	0.169	0.025	0.0053	0.067	2.02	10.8
(10 patients)	(13.8)	(0.093)	(0.012)	(0.011)	(0.0004)	(0.058)	(0.47)	(4.5)

*$p < 0.001$.
†$p < 0.05$ versus low-grade glioma.
‡$p < 0.01$.
Data shown are mean value (s.e.).
k_1^*, k_2^*, k_3^*, k_4^* = rate constants in FDG kinetic model.

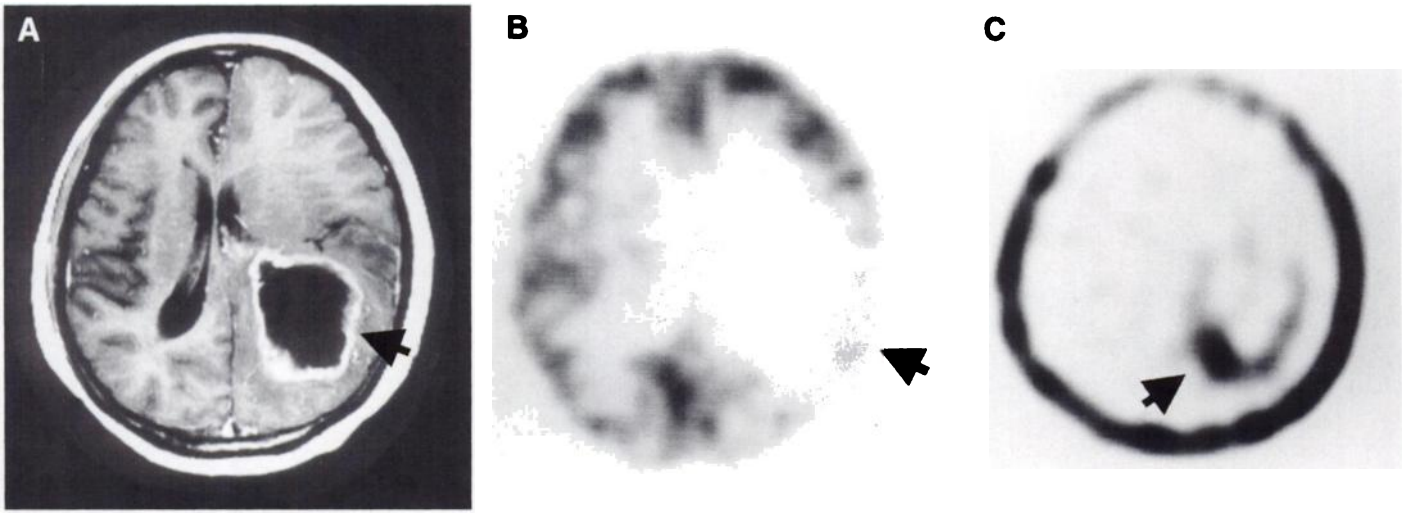

FIGURE 1. Brain scans from a 56-yr-old man with glioblastoma multiforme (Patient 2). (A) Gd-enhanced Tl-weighted MRI scan shows a tumor with well-defined thin rim and central necrosis (arrow). (B) FDG-PET scan shows a large area of defect in the left parietal subcortex. Glucose uptake in the viable rim is not demonstrated, probably due to low low contrast of radioactivity between viable tumor and adjacent normal brain and to spatial resolution. Thallium-201 SPECT shows ring-like uptake in the lesion. The highest radioactivity within the tumor is seen on the posteromedial margin, where the ROIs were placed both on the SPECT and PET images (arrows).

The rCMRgl value was increased in high-grade compared with low-grade glioma, but there was no statistically significant difference between them. Di Chiro et al. (*16*) showed that the glucose utilization rate had a positive correlation with the histological malignancy of glioma, but contradictory results have been reported by others (*26,27*). The FDG accumulation and phosphorylation does not appear to be strongly related to the proliferative activity of brain tumors (*28,29*).

There are several limitations of FDG-PET in the diagnosis of brain tumors. One major limitation is FDG uptake in normal brain tissue, such as the cortical region, thalami and basal ganglia. The rCMRgl value in most brain tumor is lower than that in normal gray matter (*30*). In in vitro experiments using the adenocarcinoma cell line, FDG uptake did not correlate with the proliferative rate but with the number of viable tumor cells (*31*). A microautoradiographic study (*32*) revealed that increased FDG uptake was caused by prenecrotic cells surrounding necrotic areas because of an altered permeability of injured cell membranes. These findings indicated that FDG was taken up by both nonproliferating and proliferating viable cells (*33*), and rCMRgl values did not always represent the malignancy of the brain tumor.

The ^{201}Tl index, however, significantly correlated with the malignancy of glioma because of the difference in biologic behavior between FDG and ^{201}Tl in brain tumor as well as background radioactivity in normal brain tissue. Thallium-201 uptake by the malignant brain tumor was much greater than that in the nonneoplastic tissues with a disrupted blood-brain barrier, such as occurs in infection and infarction (*34–37*), and normal brain tissue showed little ^{201}Tl uptake. Thallium-201 SPECT clearly delineated high-grade glioma and differentiated it from low-grade glioma. The rCMRgl value was also dependent on the lumped constant of the tumor as well as on glucose metabolism (*38–40*). The lumped constant of normal brain tissue was approximated to be uniform and insensitive to the physiological state (*41*). The lumped constant of the tumor was not measured in patients, and the measurement of rCMRgl in the brain tumor by FDG-PET studies seemed to be much more complex and variable.

The FDG rate constants were calculated by kinetic analysis

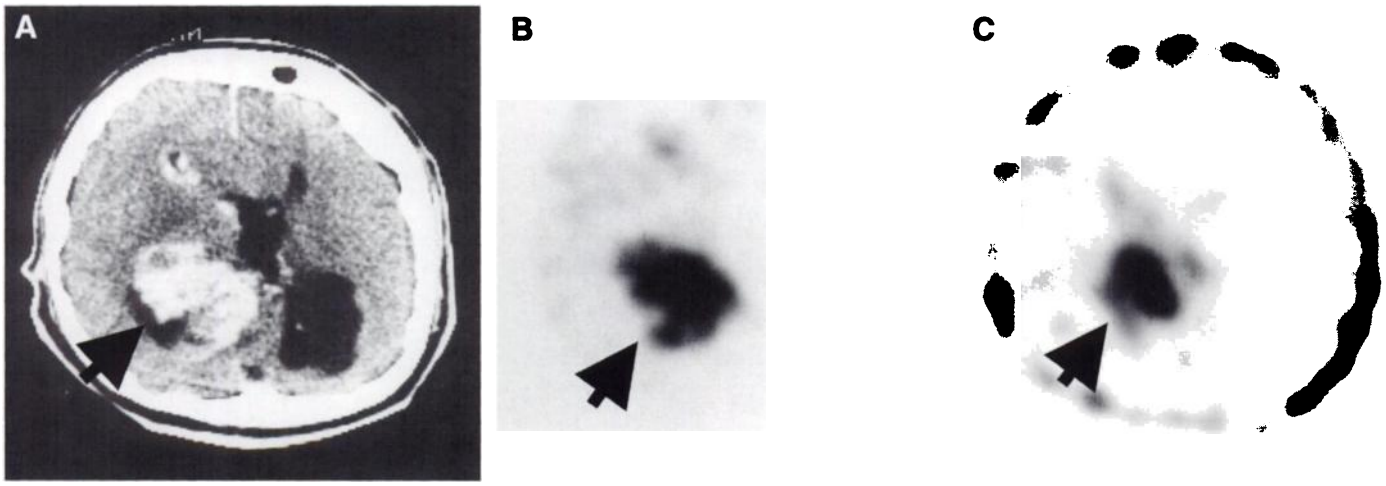

FIGURE 2. Brain scans from a 20-yr-old man with glioblastoma multiforme (Patient 3). (A) CT scan after contrast injection shows inhomogeneous enhancement of the tumor (arrow). (B) FDG-PET shows markedly increased and slightly inhomogeneous glucose uptake in the tumor (arrow). (C) Thallium-201 SPECT shows increased uptake in the tumor. Radioactivity is more increased in the central portion and is relatively homogeneous probably due to the limited spatial resolution of SPECT (arrow).

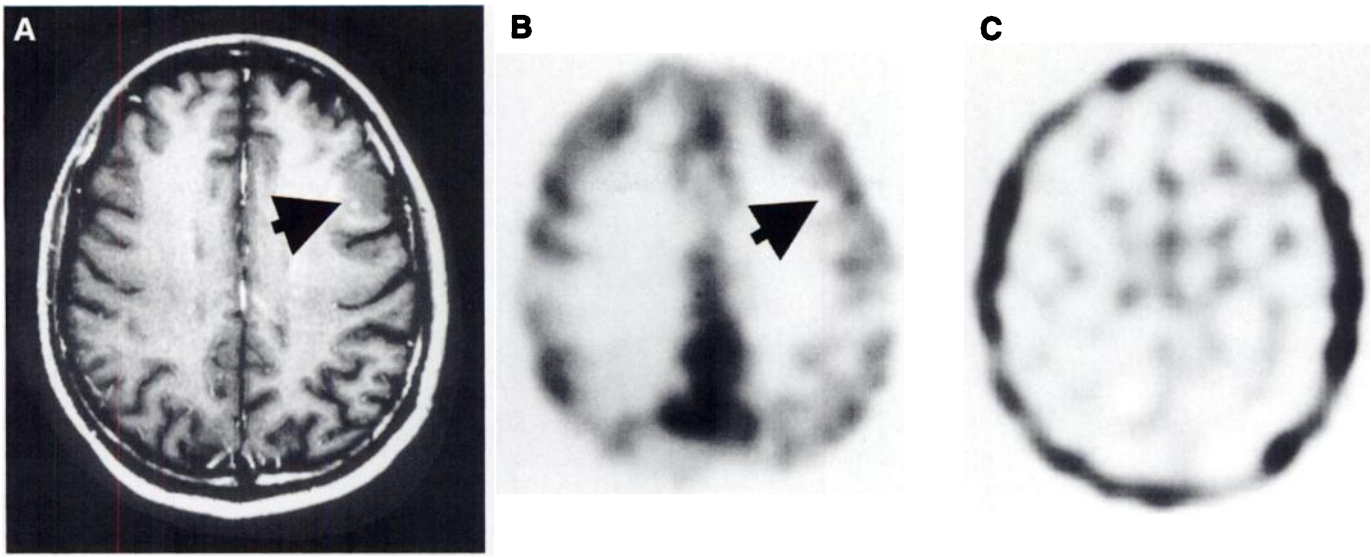

FIGURE 3. Brain scans from a 54-yr-old man with low-grade glioma (Patient 17). (A) Gd-enhanced Tl-weighted MRI scan shows nonenhancing tumor in the left temporal cortex (arrow). (B) FDG-PET scan shows no increased or decreased glucose uptake in the lesion (arrow). The rCMRgl value of the tumor is as high as surrounding that in normal brain. (C) Thallium-201 SPECT shows no increased uptake in the tumor.

using dynamic PET studies to estimate rCMRgl in brain tumor. In normal brain tissue, the rCMRgl value was calculated using fixed rate constants determined in normal volunteers by the autoradiographic method (*22,24*). FDG transport, however, between plasma and tissue and FDG metabolism in brain tumor were considered different from that in normal brain tissue (*42,43*). In the present study, we used the four-parameter kinetic model to determine the rate constants and rCMRgl in glioma. Ishikawa et al. (*44*) evaluated glucose transport in malignant glioma using dynamic PET studies and found lower transfer rate constants k_1^* and k_3^* and rCMRgl values in low-grade than in high-grade glioma. They also observed a difference in the distribution volume $k_1^*/(k_2^* + k_3^*)$ between low- and high-grade glioma (*45*). Herholz et al. (*46*) reported that the ratio of k_3^* in tumors to k_3^* in tumor-free brain significantly correlated with histological tumor grade. The present study showed no statistical significance among rate constants k_1^* and k_3^*, distribution volume $k_1^*/(k_2^* + k_3^*)$ and histological malignancy of glioma. Other rate constants also showed no significant correlation. The large variability of rate constants within each specific grade of glioma yielded large standard errors of rCMRgl values.

Both ^{201}Tl and FDG were taken up in a heterogeneous manner in gliomas, which had a heterogeneous histological appearance and were often necrotic. To minimize the variability in both ^{201}Tl and FDG uptake in the tumor, we used the average counts per pixel in the tumor to calculate the ^{201}Tl index and FDG rate constants. If the tumor had a large necrotic or cystic component, the ROI was placed on the rim of the tumor. If, however, the spatial resolution of SPECT and PET was relatively poor, the presence of small necrotic foci might not be detected, and a thin rim of the tumor around a cystic/necrotic center might not be adequately resolved. In our series, 4 of 10 patients with low-grade glioma had thin rim of less than 3 mm, and both ^{201}Tl index and rCMRgl values might have been underestimated by a partial volume effect in these patients. When there was no ^{201}Tl uptake in the tumor, the ROI was placed on the tumor site with the CT or MRI reference. The co-registration of anatomic and radionuclide images may help to improve both the visual interpretation and quantitative analyses like the ^{201}Tl index and rCMRgl values, especially when the tumor does not show high uptake compared with that in adjacent regions.

Both ^{201}Tl and FDG are known to be accumulated in various

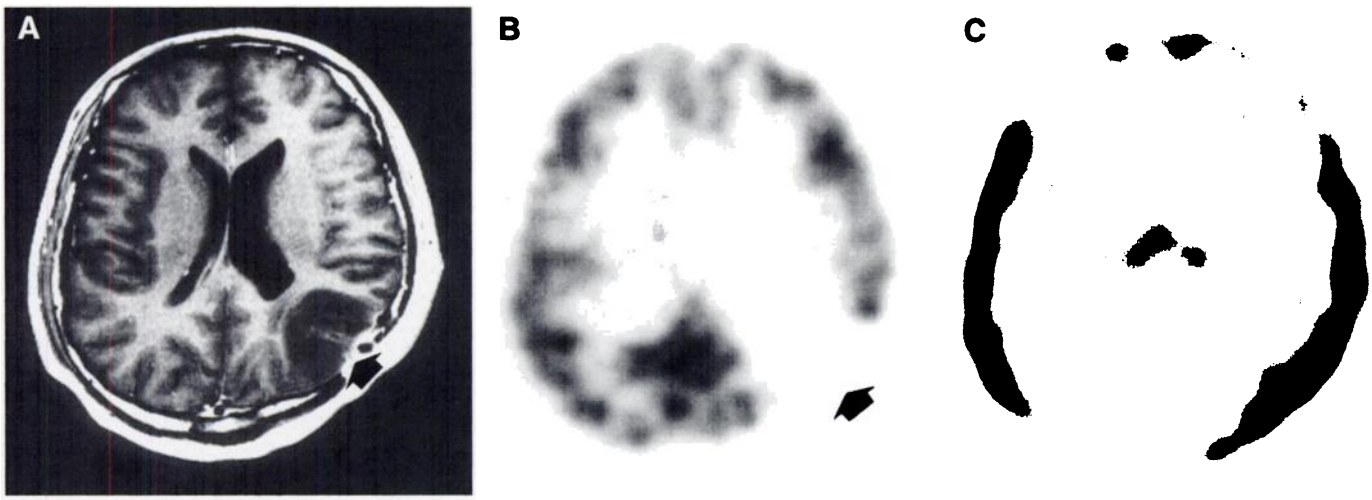

FIGURE 4. Brain scans from a 26-yr-old man with low-grade glioma (Patient 13). (A) Gd-enhanced Tl-weighted MRI scan shows a nonenhanced hypointensity area in the left temporo-occipital cortex (arrow). (B) FDG-PET shows a defect area in the lesion (arrow). (C) Thallium-201 SPECT shows no increased uptake in the lesion.

benign lesions, yielding false-positive results. Thallium-201 is taken up in areas of infection, infarction and radiation necrosis (*34–37*) and FDG in areas of abscess (*47*). Recent studies have shown the relative advantages of both FDG and ^{201}Tl in distinguishing radiation necrosis from tumor recurrence (*37,47*). A nonenhanced lesion, however, is sometimes undetectable by FDG-PET, as shown in Figure 3. Contrast enhancement on CT or MRI was demonstrated in cases of low-grade glioma. In our series, 5 of 10 cases showed enhancement. These modalities are complementary in the diagnosis of glioma.

As previously reported (*7*), follow-up ^{201}Tl brain SPECT studies were useful in determining the presence of malignant transformation. In the present study, 4 of 10 patients with low-grade glioma died. One patient (Patient 11) had lupus pneumonitis and died 3 months after SPECT/PET study. Histological diagnosis of this patient's tumor was made by stereotactic biopsy, and inadequate biopsy sampling was suspected. The other three patients manifested malignant transformation of their gliomas. Two of them (Patients 12 and 16) underwent a second SPECT study and showed increased ^{201}Tl uptake by the tumor (175% in Patient 12, 157% in Patient 16), and both died 8 and 12 months afterward, respectively. Thallium-201 SPECT and FDG-PET studies were also useful for the diagnosis of malignant transformation.

CONCLUSION

The present study demonstrated the ability of ^{201}Tl brain SPECT to diagnose the malignancy of pretreated glioma compared with FDG-PET and also showed that ^{201}Tl uptake in the tumor is independent of increased glucose transport or metabolism. Thallium-201 SPECT and FDG-PET are complementary in the diagnosis of glioma. Our results, however, are based on studies in only 20 patients and are thus preliminary. Further studies in a larger series of patients should be conducted to confirm the diagnostic relevance of both ^{201}Tl SPECT and FDG-PET.

REFERENCES

1. Salvatore M, Carratu L, Porta E. Thallium-201 as a positive indicator for lung neoplasms: preliminary experiments. *Radiology* 1976;121:487–488.
2. Cox PH, Belfer AJ, van der Pompe WB. Thallium 201 chloride uptake in tumors, a possible complication in heart scintigraphy. *Br J Radiol* 1976;49:767–768.
3. Tonami N, Hisada K. Clinical experience of tumor imaging with ^{201}Tl-chloride. *Clin Nucl Med* 1977;2:75–81.
4. Fukuchi M, Tachibana K, Kuwata K, et al. Thallium-201 imaging in thyroid carcinoma—appearance of a lymph node metastasis. *J Nucl Med* 1978;19:195–196.
5. Ancri D, Bassett JY. Diagnosis of cerebral lesions by thallium-201. *Radiology* 1978;128:417–422.
6. Ancri D, Bassett JY. Diagnosis of cerebral metastases by thallium-201. *Br J Radiol* 1980;53:443–445.
7. Oriuchi N, Tamura M, Shibazaki T, et al. Clinical evaluation of thallium-201 SPECT in supratentorial gliomas: relation to histologic grade, prognosis and proliferative activities. *J Nucl Med* 1993;34:2085–2089.
8. Black KL, Hawkins RA, Kim KT, et al. Use of thallium-201 SPECT to quantitate malignancy grade of gliomas. *J Neurosurg* 1989;71:342–346.
9. Kim KT, Black KL, Marciano D, et al. Thallium-201 SPECT imaging of brain tumors: methods and results. *J Nucl Med* 1990;31:965–969.
10. Mountz JM, Stafford-Schuck K, McKeever PE, et al. Thallium-201 tumor/cardiac ratio estimation of residual astrocytoma. *J Neurosurg* 1988;68:705–709.
11. Gehring PJ, Hammond PB. The interrelationship between thallium and potassium in animals. *J Pharmacol Exp Ther* 1967;155:187–201.
12. Atkins HL, Budinger TF, Lobowitz E, et al. Thallium-201 for medical use. Part 3: human distribution and physical imaging properties. *J Nucl Med* 1977;18:133–140.
13. Kaplan WD, Takvorian T, Morris JH, et al. Thallium-201 brain tumor imaging: a comparative study with pathologic correlation. *J Nucl Med* 1987;28:47–52.
14. Kasarov LB, Fiedman H. Enhanced Na^+-K^+ activated adenosine triphosphatase activity in transformed fibroblasts. *Cancer Res* 1974;34:1862–1865.
15. Elligsen JD, Thompson JE, Frey HE, et al. Correlation of (Na^+-K^+) ATPase activity with growth of normal and transformed cells. *Exp Cell Res* 1974;87:233–240.
16. Di Chiro G, DeLaPaz RL, Blooks RA, et al. Glucose utilization of cerebral gliomas measured by [^{18}F]fluorodeoxyglucose and positron emission tomography. *Neurology* 1982;32:1323–1329.
17. Di Chiro G, Hatazawa J, Katz DA, et al. Glucose utilization by intracranial meningiomas as an index of tumor aggressivity and probability of recurrence: a PET study. *Radiology* 1987;164:521–526.
18. Patronas NJ, Di Chiro G, Kufta C, et al. Prediction of survival in glioma patients by PET. *J Neurosurg* 1986;62:816–822.
19. Alavi JB, Alavi A, Chawluk J, et al. Positron emission tomography in patients with glioma: a predictor of prognosis. *Cancer* 1988;62:1074–1078.
20. Doyle WK, Budinger TF, Levin VA, et al. Differentiation of cerebral radiation necrosis from tumor recurrence by ^{18}F-FDG and Rb-82 positron emission tomography. *J Comput Assist Tomogr* 1987;11:563–570.
21. Ogawa T, Uemura K, Shishido F, et al. Changes of cerebral blood flow, oxygen and glucose metabolism following radiochemotherapy of gliomas: a PET study. *J Comput Assist Tomogr* 1988;12:290–297.
22. Phelps ME, Huang SC, Hoffman EJ, Selin C, Sokoloff K, Kuhl DE. Tomographic measurement of local cerebral glucose metabolic rate in humans with (F-18) 2-fluoro-2-deoxy-D-glucose: validation of method. *Ann Neurol* 1979;6:371–388.
23. Hawkins RA, Phelps ME, Huang SC. Effects of temporal sampling, glucose metabolic rates and distribution of the blood-brain barrier on the FDG model with and without a vascular component: studies in human brain tumors with PET. *J Cereb Blood Flow Metab* 1986;6:170–183.
24. Reivich M, Kuhl A, Wolf A, et al. The [^{18}F]fluorodeoxyglucose method for the measurement of local cerebral glucose utilization in man. *Circ Res* 1979;44:127–137.
25. Slizofski WJ, Krishna L, Katsetos CD, et al. Thallium imaging for brain tumors with results measured by a semiquantitative index and correlated with histopathology. *Cancer* 1994;74:3190–3197.
26. Tyler JL, Diksic M, Villemure J-D, et al. Metabolic and hemodynamic evaluation of gliomas using positron emission tomography. *J Nucl Med* 1987;28:1123–1133.
27. Herscovitch P, Raichle M. Effect of tissue heterogeneity on the measurement of cerebral blood flow with the equilibrium $C^{15}O_2$ inhalation technique. *J Cereb Blood Flow Metab* 1983;3:407–415.
28. Minn H. Fluorodeoxyglucose imaging: a method to assess the proliferative activity of human cancer in vivo: comparison with DNA flow cytometry in head and neck tumors. *Cancer* 1988;61:1776–1781.
29. Haberkorn U, Strauss L, Reisser C, et al. Glucose uptake, perfusion and cell proliferation in head and neck tumors: relation of positron emission tomography to flow cytometry. *J Nucl Med* 1991;32:1548–1555.
30. Mineura K, Sasajima T, Kowada M, et al. Perfusion and metabolism in predicting the survival of patients with gliomas. *Cancer* 1994;73:2386–2394.
31. Higashi K, Clavo AC, Wahl RL. Does FDG uptake measure proliferative activity of human cancer cells? In vitro comparison with DNA flow cytometry and tritiated thymidine uptake. *J Nucl Med* 1993;34:414–419.
32. Kubota R, Kubota K, Yamada S, Tada M, Ido T, Tamahashi N. Active and passive mechanisms of [^{18}F]fluorodeoxyglucose uptake by proliferating and prenecrotic cells in vivo: a microautoradiographic study. *J Nucl Med* 1994;35:1067–1075.
33. Kubota K, Kubota R, Yamada S. FDG accumulation in tumor tissue [Editorial]. *J Nucl Med* 1993;34:419–421.
34. Tonami H, Matsuda H, Ooba H, et al. Thallium-201 accumulation in cerebral candidiasis. *Clin Nucl Med* 1990;15:397–400.
35. Krishna L, Slizofski WJ, Katsetos CD, et al. Abnormal intracerebral thallium localization in a bacterial brain abscess. *J Nucl Med* 1992;33:2017–2019.
36. Moody EB, Hodes JE, Walsh JW, Thornsberry S. Thallium avid cerebral radiation necrosis. *Clin Nucl Med* 1994;19:611–613.
37. Buchpigueli CA, Alavi JB, Alavi A, Kenyon LC. PET versus SPECT in distinguishing radiation necrosis from tumor recurrence in the brain. *J Nucl Med* 1995;36:159–164.
38. Gjedde A, Wienhard KK, Heiss WD, et al. Comparative regional analysis of 2-fluoro deoxyglucose and methyl glucose uptake in brain of four stroke patients with special reference to the regional estimation of the lumped constant. *J Cereb Blood Flow Metab* 1985;5:163–178.
39. Kaper R, Spence AM, Muzi M, Graham MN, Abbott GL, Krohn KA. Determination of the deoxyglucose and glucose phosphorylation ratio and the lumped constant in rat brain and a transplantable rat glioma. *J Neurochem* 1989;53:37–44.
40. Spence A, Graham M, Muzi M, et al. Deoxyglucose lumped constant estimated in a transplanted rat astrocytic glioma by the hexose utilization index. *J Cereb Blood Flow Metab* 1991;10:190–198.
41. Sokoloff L, Reivich M, Kennedy C, et al. The [^{11}C]-deoxyglucose method for the measurement of local cerebral glucose utilization: theory, procedure and normal values in the conscious and anesthetized albino rat. *J Neurochem* 1977;28:897–916.
42. DiChiro G. Positron emission tomography using [^{18}F]fluorodeoxyglucose in brain tumors—a powerful diagnostic and prognostic tool. *Invest Radiol* 1987;22:360–371.
43. Flier JS. Elevated levels of glucose transport and transporter messenger RNA are induced by ras or src oncogenes. *Science* 1987;235:1492–1495.
44. Ishikawa M, Kikuchi H, Nishizawa S, Yonekura Y. Evaluation of glucose transport in malignant glioma by PET. *Acta Neurochir Suppl (Wien)* 1990;51:165–167.
45. Ishikawa M, Kikuchi H, Nagata I. Glucose consumption and rate constants for ^{18}F-fluorodeoxyglucose in human gliomas. *Neurol Med Chir* 1990;30:377–381.
46. Herholz K, Rudolf J, Heiss WD. FDG transport and phosphorylation in human gliomas measured with dynamic PET. *J Neurooncol* 1992;12:159–165.
47. Kahn D, Follett KA, Bushnell DL, et al. Diagnosis of recurrent brain tumor: value of ^{201}Tl SPECT versus ^{18}F-fluorodeoxyglucose PET. *Am J Roentgenol* 1994;163:1459–1465.